Experimental observation of narrow surface plasmon resonances in gold nanoparticle arrays

Yizhuo Chu, Ethan Schonbrun, Tian Yang, and Kenneth B. Crozier[a]

School of Engineering and Applied Sciences, Harvard University, Cambridge, Massachusetts 02138, USA

We demonstrate that coupling between grating diffraction and localized surface plasmons in two-dimensional gold nanoparticle arrays in water leads to narrow near-infrared resonance peaks in measured far field extinction spectra. Good agreement is obtained between finite difference time domain (FDTD) calculations and experimental extinction spectra. The FDTD calculations predict that the gold nanoparticle arrays exhibit near-field electric field intensity (E^2) enhancements approximately one order of magnitude greater than those of single isolated gold nanoparticles. © 2008 American Institute of Physics. [DOI: 10.1063/1.3012365]

Localized surface plasmon (LSP) can lead to giant enhancements of the local electromagnetic fields around nanoparticles.[1,2] In nanoparticle arrays, interactions between individual dipole plasmons can further increase the field enhancement. Meier *et al.*[3] found that strong dipolar interactions occur when a grating order changes from evanescent to radiative, which was later confirmed experimentally by Lamprecht *et al.*[4] Recently, it has been theoretically predicted that dipolar coupling in one- and two-dimensional (2D) nanoparticle arrays can produce very narrow plasmon line shapes[5] and exceptionally large electromagnetic enhancements[2] ($|E|^2 > 10^7$). Hicks *et al.*[6] measured the plasmon line shape of linear arrays of Ag nanoparticles, finding a narrow mode that gained strength for interparticle distances close to the single particle resonance wavelength. However, the experimentally measured peaks, with full width at half maximum (FWHM) values of ~50 nm, were broader than theory, which predicted FWHMs as small as 2 nm. This was attributed to the spread of illumination and collection angles in the experiment, among other factors.[6]

In this letter, we show experimentally and theoretically that dipolar coupling in two-dimensional nanoparticle arrays leads to narrow surface plasmon resonance peaks. Our extinction cross section experimental results are in good agreement with theory. Numerical modeling indicates that the field enhancement in nanoparticle arrays can be considerably larger than that in a single isolated nanoparticle. In addition, we show that, for certain nanoparticle arrays, varying the angle of incidence leads to narrower extinction spectra with larger peak values.

Gold nanoparticle arrays are fabricated by e-beam lithography on indium tin oxide (ITO)-coated glass slides, as shown in Fig. 1(a). The gold nanoparticle arrays are square lattices of gold disks with grating constants varying from 520 to 640 nm. The gold disks are 180 nm in diameter and 40 nm thick. Each array occupies a square region of 135×135 μm^2.

To model the optical properties of the nanoparticle arrays, we use the finite-difference time-domain (FDTD) method to calculate near-field intensity spectra and spatial distributions [Figs. 1(b) and 1(c)]. The medium above the glass substrate is water. The water environment enables stronger interaction between grating diffraction and single nanoparticle plasmons, resulting in a larger field enhancement than an air environment due to the reduced index contrast between water and glass. A linearly polarized plane wave illuminates the device from the glass side at normal incidence. A point monitor is placed at the edge of the gold disk at the gold-water interface to record the near-field intensity. The monitor is located such that the radial vector, from the disk center to the monitor, is along the polarization direction of the illumination. The refractive indices of glass and water are 1.517 and 1.327, respectively. A 20 nm thick layer of ITO with an index of 1.45 is simulated.[7] In Fig. 1(c), the intensity (square of electric field $\langle |E|^2 \rangle$) is plotted as a function of wavelength for a single isolated disk and for arrays of disks, both on glass in water. The intensity is normalized to the intensity that would occur in the absence of the disks. In Fig. 1(b), the intensity distributions are shown on the top surface of a single isolated disk and on a disk from a 2D array (640 nm period), respectively. The FDTD results indicate that considerably larger intensity enhancements are
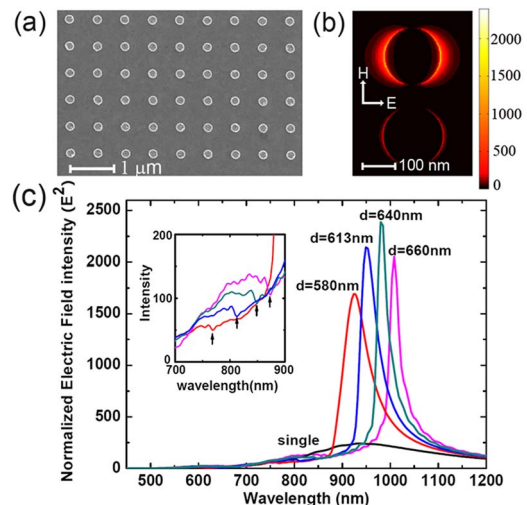

FIG. 1. (Color online) (a) Scanning electron micrograph of gold disk array. (b) Intensity ($\langle |E|^2 \rangle$) distribution on surface of single gold disk at $\lambda = 930$ nm (bottom). Intensity distribution on surface of gold disk of an array with a grating constant $d=640$ nm at $\lambda=982$ nm (top). Polarization of plane wave illumination is shown, which is along one axis of the square array. (c) Near-field intensity enhancement ($\langle |E|^2 \rangle$) spectra for a single isolated gold disk and for gold disks in 2D arrays of different grating constants (d). Inset: expanded view of near-field spectra over the range $\lambda=700–900$ nm.

[a]Electronic mail: kcrozier@seas.harvard.edu.

possible for disk arrays than for single isolated disks. From Fig. 1(c), it can be seen that the peak intensity enhancement for a single gold disk is ∼240 times. By contrast, the peak intensity enhancement for the 640 nm period gold disk array is ∼2400 times. It also can be seen that the near-field intensity resonance peak of a gold disk array can be much sharper than that of an isolated gold disk. The narrowest resonance peak of the near-field intensity spectra occurs for the grating constant of 660 nm and has a FWHM of 26.6 nm. This is more than ten times narrower than the resonance peak of an isolated gold disk, which has a FWHM of 311.6 nm.

The plasmon resonance of a single disk [black curve of Fig. 1(c)] occurs at a free-space wavelength of $\lambda_{single} \approx 930$ nm, corresponding to an effective wavelength of 613 nm in the glass substrate. In a gold disk array, diffraction results in a strong dipolar interaction when a grating order changes from evanescent to radiative.[3] The wavelengths at which this occurs are given by

$$\lambda_{(i,j)} = \frac{d \times n}{(i^2 + j^2)^{1/2}}, \qquad (1)$$

where d is the grating constant, n is either the index of water or glass, and (i,j) denotes the grating diffraction order. When the grating constant is fixed, new grating orders appear, i.e., change from evanescent to radiative, as the incident wavelength λ decreases. As noted by Lamprecht *et al.*,[4] at a wavelength λ which is slightly longer than $\lambda_{(i,j)}$, the grating order (i,j) is still evanescent and a strong dipolar interaction occurs due to the approximately in-phase addition of the fields scattered by the nanoparticles. For $\lambda = \lambda_{(i,j)}$, the grating order (i,j) begins to radiate at grazing angle. As a grating order becomes radiative, a sudden change in the amplitudes of different grating orders is expected,[3] leading to changes in the near and far fields. The first grating order in the glass substrate, for which $(i,j)=(0,1)$ or $(1,0)$, changes from evanescent to radiative at $\lambda_{glass(0,1)}=d \times n_{glass}$. Our results indicate that the resonance of a gold disk array occurs at a wavelength slightly longer than $\lambda_{glass(0,1)}$, consistent with the results of Ref. 4. Features can be seen in the near-field intensity spectra that occur close to wavelengths corresponding to the appearance of the first grating order in water. These wavelengths, calculated using $\lambda_{water(0,1)}=d \times n_{water}$, are denoted by black arrows in the inset of Fig. 1(c). To maximize the electromagnetic enhancement, we tuned the grating constant d to be 613 nm so that $\lambda_{glass(0,1)}=930$ nm, which matches the single disk plasmon resonance. However, our FDTD simulations indicate that the largest enhancement occurs for a grating constant of 640 nm rather than 613 nm. We believe that this is due to the plasmon resonance shifting as a result of dipolar coupling between the gold disks.

To observe the effect of this phenomenon on the extinction cross section, we carry out transmission measurements on fabricated devices. A collimated and polarized beam is incident on the sample, with the transmitted light collected by a microscope objective (50×, numerical aperture of 0.45). The polarization is along one of the axes of the square lattice. An iris placed at the image plane of the objective ensures that only the light transmitted by the array is coupled into a spectrometer. The extinction cross section C_{ext} of each gold disk of the array is found from the transmission T using the relation: $T=1-C_{ext}/d^2$, where d is the grating constant.
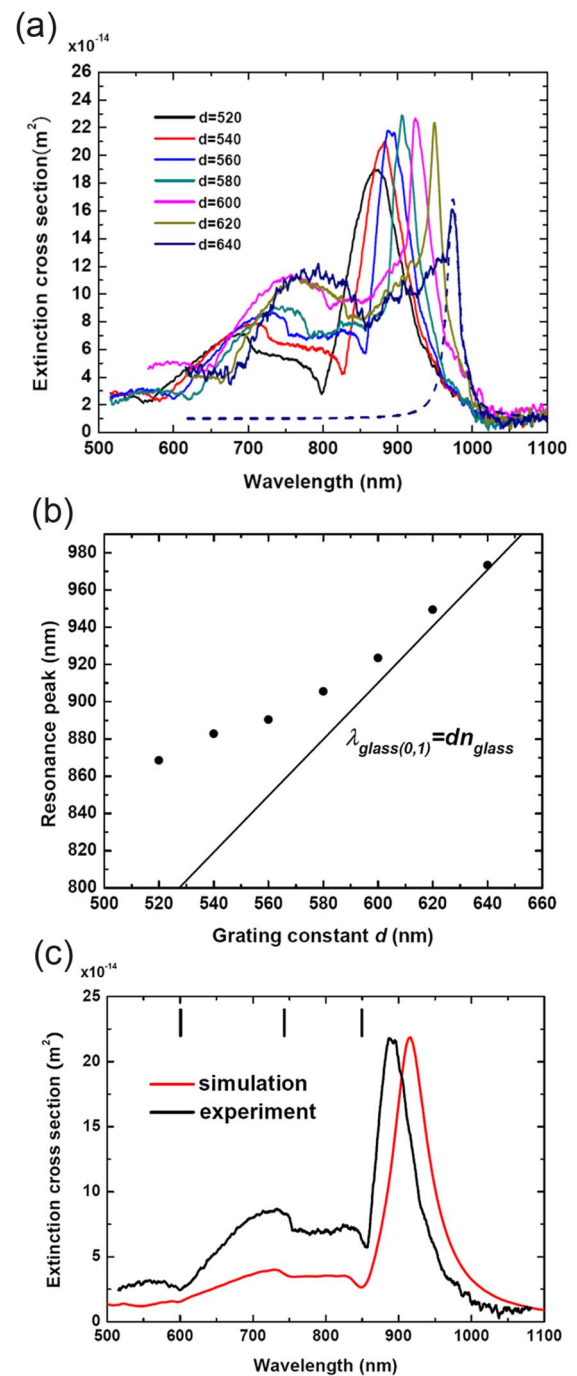

FIG. 2. (Color online) (a) Measured extinction spectra of gold disk arrays in water (solid lines) and the Lorentzian fit of the extinction peak (dashed line). (b) Peak positions of the extinction peaks (dots) and the first grating order in glass $\lambda_{glass(0,1)}=d \times n_{glass}$ (solid line). (c) Measured and calculated transmission spectra of gold disk array with a grating constant of 560 nm.

This can be understood by considering that zero transmission would occur should C_{ext} be equal to the area of the unit cell d^2. The sample is rotated such that the polarization direction is along the axis of rotation. At angled incidence, C_{ext} is calculated using $T=1-C_{ext}/(d^2 \cos \theta)$, where θ is the angle between the wavevector of the illumination and the normal to the sample.

In Fig. 2(a), the measured extinction cross section spectra are plotted for gold disk arrays in water with different grating constants d. The grating constant clearly plays a strong role in the peak value and peak position of the extinc-

tion cross section. The resonance peak position is plotted as a function of grating constant in Fig. 2(b). As discussed above, the resonance peaks occur at wavelengths slightly redshifted from $\lambda_{glass(0,1)}$. It can be seen that the peak position becomes closer to $\lambda_{glass(0,1)}$ for the samples having longer grating constants. In addition, as discussed further below, for the samples with grating constants of 520, 540, and 560 nm, while the peak position is redshifted from $\lambda_{glass(0,1)}$, the spectra exhibit dips close to $\lambda_{glass(0,1)}$. Measured and FDTD-calculated extinction spectra of 560 nm period gold disk arrays are shown in Fig. 2(c). The FDTD-calculated extinction spectrum is obtained using a planar monitor in the far field (40 μm away from the array), which records the power flow through the area of the simulated cell. Good agreement is observed between the experiments and the FDTD simulations, with some differences that could be due to the fabrication imperfections and/or uncertainties in the refractive indices of the gold, water, glass substrate, and ITO layer. Each solid mark represents the wavelength at which a grating order changes from evanescent to radiative, as found from Eq. (1). As discussed above, features in the extinction cross section spectra occur with the appearance of each new grating order. From Fig. 2(c), a dip in the spectrum occurs at $\lambda \sim 855$ nm, close to the wavelength at which a grating order becomes radiative. This wavelength is denoted as $\lambda_{glass(0,1)}$ in Fig. 2(b). From Fig. 2(a), it can also be seen that for a grating constant of 580 nm, the extinction peak has the maximum value. To measure the width of the extinction peak, we use a Lorentzian line shape in the frequency domain

$$L(f) = L_0 + \frac{2A}{\pi}\left[\frac{w}{4(f-f_0)^2 + w^2}\right] \tag{2}$$

to fit the peaks, where f is the frequency, f_0 is the peak position, and w is the FWHM in frequency. The FWHM in wavelength is calculated from w and f_0. Because of the multiple features on the shorter-wavelength side of the main extinction peak arising from the appearance of new grating orders, we only use the top part and the longer-wavelength side of the peaks in the fitting. The dashed line in Fig. 2(a) shows the result of the fitting for the array with grating constant of 640 nm. The array with the grating constant of 640 nm has the narrowest extinction peak, with a FWHM in wavelength of 19.8 nm. The simulations predict that the highest peak in the far field spectra (not shown) occurs for a grating constant of 620 nm, which is longer than the extinction cross section experimental result, for which the array with a grating constant of 580 nm has the largest peak extinction cross section. This is possibly due to the imperfect shape of the fabricated disks.

In Fig. 3, the spectra are shown for measurements made on the 540 nm period array with the angle of incidence varied from 0° to 14°. As the incident angle increases, the peak becomes sharper and higher at first, and then broader and smaller for angles greater than 8°. It can be shown that the first diffraction order into glass is tangential to the grating plane at $\lambda_{glass(0,1),\theta}=d \times n_{glass}+d \times n_{air} \times \sin \theta$. Similar to the normal incidence case, the resonance occurs at the wavelength slightly longer than $\lambda_{glass(0,1)}$. At normal incidence, $\lambda_{glass(0,1)}$ of an array with a grating constant of 540 nm is
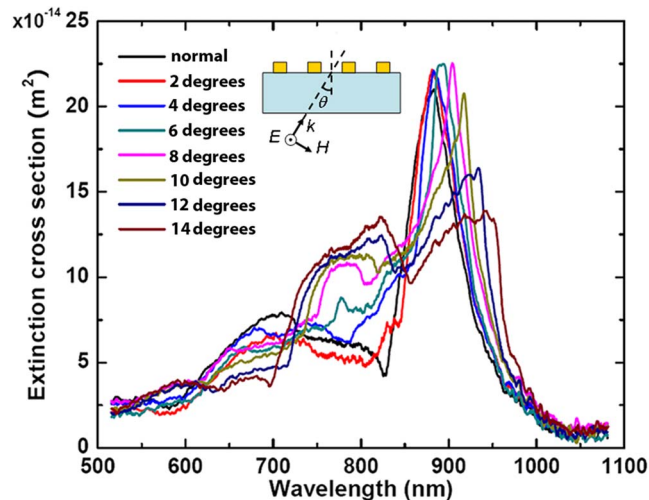

FIG. 3. (Color online) Extinction spectra of gold disk arrays with an angle of incidence varied. Grating constant: $d=540$ nm. Inset: Sketch of the angular incidence. The polarization direction is parallel to the array.

shorter than the plasmon resonance of a single disk with a diameter of 180 nm. One can tune $\lambda_{glass(0,1)}$ to match with the single disk plasmon resonance by increasing the angle of incidence. This should result in a larger and narrower extinction cross section, with corresponding greater near-field intensity enhancement. The extinction peak reaches its maximum value for the incident angle of 8°, corresponding to $\lambda_{glass(0,1),8}=894.3$ nm. The value of $\lambda_{glass(0,1),8}$ is close to that of the normal incidence case in which the array with a grating constant of 580 nm has the highest extinction peak, corresponding to $\lambda_{glass(0,1)}=879.8$ nm. This demonstrates that for the samples in which $\lambda_{glass(0,1)}$ mismatches with the single disk resonance at normal incidence, changing the incident angle allows the coupling between dipoles to be increased.

In summary, we observe sharp resonances in the extinction cross sections when the product of the grating constant and the substrate refractive index approximately matches the single disk resonance at normal incidence. The larger field enhancement, as predicted by FDTD, could be important for surface enhanced Raman spectroscopy and biosensors and biosensors.

See also related work by Auguie and Barnes,[8] published after the submission of this letter.

[1] E. Hao and G. C. Schatz, J. Chem. Phys. **120**, 357 (2004).
[2] S. Zou and G. C. Shatz, Chem. Phys. Lett. **403**, 62 (2005).
[3] M. Meier, A. Wokaun, and P. F. Liao, J. Opt. Soc. Am. B **2**, 931 (1985).
[4] B. Lamprecht, G. Schider, R. T. Lechner, H. Ditlbacher, J. R. Krenn, A. Leitner, and F. R. Aussenegg, Phys. Rev. Lett. **84**, 4721 (2000).
[5] S. Zou, N. Jarel, and G. C. Schatz, J. Chem. Phys. **120**, 10871 (2004).
[6] E. M. Hicks, S. Zou, G. C. Schatz, K. G. Spears, R. P. Van Duyne, L. Gunnarsson, T. Rindzevicius, B. Kasemo, and M. Kall, Nano Lett. **5**, 1065 (2005).
[7] D. E. Groom, S. E. Holland, M. E. Levi, N. P. Palaio, S. Perlmutter, R. J. Stover, and M. Wei, Proc. SPIE **3649**, 80 (1999).
[8] B. Auguié and W. L. Barnes, Phys. Rev. Lett. **101**, 143902 (2008).